

A Potential Based Panel Method for Prediction of Steady and Unsteady Performances of Contra-rotating Propellers

Liu Xiao-long

China Ship Scientific Research Center(CSSRC), Wuxi, China

ABSTRACT

A numerical procedure is developed to predict the steady and unsteady performances of contra-rotating propellers in this paper, in which a potential based panel method is applied for the flow around fore propeller together with aft propeller respectively. The interaction among them is treated in an iterative manner. To facilitate the computation, circumferentially averaged values of the induced velocities are applied to consider the steady hydrodynamic interaction between fore propeller and aft propeller. The unsteady hydrodynamic interaction between them is solved by an iterative method in the time domain. In addition, a time marching method for the unsteady interaction of vortex shedding of two propellers. Programs for the fore propeller and the aft one are run by turns until convergent results of hydrodynamic forces for each part are obtained. Numerical calculations are conducted for two examples. Comparisons of some numerical results with the experimental data show good agreement.

Keywords

Contra-rotating propellers; Steady; Unsteady; Panel method

1 INTRODUCTION

The contra-rotating propellers(CRPs) have been widely used in modern ships on account of their high efficiency. The two blade rows of CRPs rotate in opposite directions, so CRPs can be designed to cancel the total swirl downstream to provide the high efficiency. On the other hand, CRPs also torque balanced, which is important for vessels which need accurate positioning.

Extensive publications may be found on the subject of CRPs, such as design method, prediction method and experiment. Tsakonas applied linearized unsteady lifting surface theory to predict steady/unsteady loads and hydrodynamic forces in the paper(Tsakonas et al 1983).Yang also applied a lifting surface method by considering the interactions between the trailing vortex sheets of the two blade rows(Yang et al 1991&1992). Gu and Kinnas coupled a Vortex-Lattice Method(VLM) applied to each of the blade rows of the CRPs or the propeller inside the duct, with a Finite Volume Method(FVM) based Euler solver applied to the global

flow-field, in order to account for the interactions between the two blade rows, in the case of a CRPs, and between the propeller and the surrounding duct, in the case of a ducted propeller(Gu & Kinnas 2003). Miller carried experiments of unsteady forces on CRPs in uniform and non-uniform flow(Miller 1976&1981). M.Strasberg studied the frequencies of the alternating forces due to interactions of CRPs(M.Strasberg & Breslin 1976).Hoshino applied the unsteady propeller lifting surface theory based on quasi-continuous method to analyze propeller shaft forces of CRPs and compared the prediction results with model and full scale data in three conditions of straight run, port turning and starboard turning(Hoshino 1994).

In this paper, a potential based panel method is employed for solving the hydrodynamic performance of the fore propeller and the aft one. To facilitate the computation, circumferentially averaged values of the induced velocities are adopted to consider the steady hydrodynamic interaction of the two blade rows. The unsteady hydrodynamic interaction of them is solved by an iterative method in the time domain, in which a time marching processing method for the unsteady interaction of vortex shedding is applied for the fore propeller and the aft one.

2 FORMULATIONS

Consider CRPs working in an unbounded flow field. The fluid is assumed to be inviscid and incompressible. A Cartesian coordinate system fixed in space $O-XYZ$ is applied, shown in Figure.1. X -axis coincides with the shaft axis of propeller and points downstream. The Z -axis points vertically upwards and the Y -axis completes the right-handed system. A second coordinate system fixed in the fore propeller $o-x_1y_1z_1$. The inflow \vec{V}_1 is along the x_1 -axis. The propeller blades rotate around x_1 -axis at a constant angular velocity Ω_1 . A third coordinate system fixed in the aft propeller $o'-x_2y_2z_2$. The inflow \vec{V}_1 is along the x_2 -axis. The aft blades rotate around x_2 -axis at a constant angular velocity Ω_2 .The distance between the origins O and O' is the axial spacing X_D . The three coordinate systems are shown in Figure.1. The corresponding formulas are listed in equations (1) and

(2). The subscript $i=1$ denotes the fore propeller, $i=2$ for the aft one; $\lambda_i=1$ denotes the left rotation, $\lambda_i=2$ for the right rotation.

$$\begin{cases} X = x_i + (i-2)x_D \\ Y = y_i \cdot \cos(\lambda_i \Omega_i t) - z_i \cdot \sin(\lambda_i \Omega_i t) \\ Z = y_i \cdot \sin(\lambda_i \Omega_i t) + z_i \cdot \cos(\lambda_i \Omega_i t) \end{cases} \quad (1)$$

$$x_i = x_i, y_i = -r_i \cdot \sin \theta_i, z_i = r_i \cdot \cos \theta_i \quad (2)$$

Where $r_i = \sqrt{y_i^2 + z_i^2}$, $\theta_i = \tan^{-1}(-y_i / z_i)$.

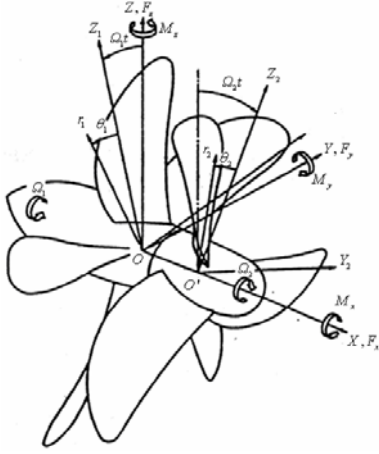


Figure.1 Coordinate system of Contra-rotating propellers

For the steady case, a set of linear algebraic equations for unknown doublet strengths on the fore propeller can be written as follows:

$$\sum_{j=1}^{N_F} (\delta_{ij} - C_{ij}) \phi_j - \sum_{m=1}^{N_{WF}} W_{im} \Delta \phi_m = - \sum_{j=1}^{N_F} B_{ij} (\vec{V}_I + \vec{V}_{FA})_j \cdot \vec{n}_{Fj} \quad i=1,2,\dots,N_F \quad (3-a)$$

For the unsteady case, similar to the unsteady performance prediction of single propeller, the resulting simultaneous equations for unknown doublet strengths on the fore propeller at each time step $n = t / \Delta t$ can be expressed as:

$$\begin{aligned} \sum_{j=1}^N (\delta_{ij} - C_{ij}) \phi_j(n) - \sum_{m=1}^{N_{WF}} W_{im} \Delta \phi_m(n) = \\ - \sum_{j=1}^N B_{ij} (\vec{V}_I(n) + \vec{V}_{FA}(n))_j \cdot \vec{n}_{Fj} + \sum_{m=1}^{N_{WF}} \sum_{l=2}^{N_{FL}} W_{iml} \Delta \phi_{ml}(n) \end{aligned} \quad i=1,2,\dots,N \quad (3-b)$$

Where $N=KN_F$ is total number of control points of the whole fore propeller, N_F denotes the total number of the control points on one blade of the fore propeller together with hub part between two adjacent blades and K is the number of the fore propeller blades. N_{WF} is the number of strips behind training edges of one blade and the number of all blades for unsteady case respectively. N_{FL} is the number of panels on one strip behind the training edge. ϕ_j and $\phi_j(n)$ designate the doublet strengths of j -th panel on the propeller blade for the steady case and unsteady case at time step n respectively. $\Delta \phi_m$ is the strength of the doublet allocated on the wake strips of the propeller for

the steady case and $\Delta \phi_{ml}(n)$ is the doublet strength at l -th panel on the m -th strip of propeller training vortex sheet at time step n . C_{ij} , W_{im} , W_{iml} and B_{ij} are influence coefficients. $\vec{V}_I(n)$ is the velocity of incoming flow relative to the propeller. $\vec{V}_{FA}(n)$ is induced velocity on the fore propeller control points due to the aft one. The strength of shedding vortex in equation (3-b) can be determined by

$$\begin{cases} \Delta \phi_{ml}(x, y, z, n) = \Delta \phi_{ml}(x, y, z, n-l+1); & l \geq 2; n \geq l \\ \Delta \phi_{ml}(x, y, z, n) = \Delta \phi_m^s(x, y, z); & l \geq 2; n < l \end{cases} \quad (4)$$

in which $\Delta \phi_m^s(x, y, z)$ denotes the potential of training vortex sheet of the propeller under steady condition.

In order to eliminate the influence of time step upon the calculated results, the doublet strength at first panel on the training vortex sheet $\Delta \phi_{m1}(x, y, z, n)$ is obtained by using linearization treatment as follows:

$$\Delta \phi_{m1}(x, y, z, n) = \frac{\Gamma_m(n) + \Gamma_m(n-1)}{2} \quad (5)$$

Where $\Gamma_m(n)$ stands for the circulation around the m -th strip of the propeller blade at time step n .

In the same way, the corresponding two sets of linear simultaneous equations for unknown doublet strengths on the aft propeller for the steady and unsteady cases

$$\sum_{j=1}^{N_A} (\delta_{ij} - C_{ij}) \phi_j - \sum_{m=1}^{N_{WA}} W_{im} \Delta \phi_m = - \sum_{j=1}^{N_A} B_{ij} (\vec{V}_I + \vec{V}_{AF})_j \cdot \vec{n}_{Aj} \quad i=1,2,\dots,N_A \quad (6-a)$$

$$\begin{aligned} \sum_{j=1}^{N_A} (\delta_{ij} - C_{ij}) \phi_j(n) - \sum_{m=1}^{N_{WA}} W_{im} \Delta \phi_m(n) = \\ - \sum_{j=1}^{N_A} B_{ij} (\vec{V}_I(n) + \vec{V}_{AF}(n))_j \cdot \vec{n}_{Aj} + \sum_{m=1}^{N_{WA}} \sum_{l=2}^{N_{AL}} W_{iml} \Delta \phi_{ml}(n) \end{aligned} \quad i=1,2,\dots,N \quad (6-b)$$

Meanings of notation of the variables in equations (6-a) and (6-b) can be easily understood. Only should $\vec{V}_{AF}(n)$ be emphasized, which denotes the induced velocities on the aft propeller due to the fore one.

The equal pressure Kutta condition is applied at the training edge of two blade rows and is expressed as

$$\Delta p_m(n) = p_{TE_m}^+(n) - p_{TE_m}^-(n) = 0, m=1,2,\dots,N_{STRIP} \quad (7)$$

in which $p_{TE_m}^+(n)$ and $p_{TE_m}^-(n)$ denote the pressure of upper side and the pressure of lower side of trailing edge at each time step n respectively. The equal pressure Kutta condition should be fulfilled at each time step n for the unsteady case. N_{STRIP} denotes the number of wake strips behind training edges of two blade rows.

A modified trailing vortex wake model of propeller, as shown in Figure.2, is adopted to describe the deformation of trailing vortex sheet(Wang & Hu 1988).

Three sets of linear algebraic equations (3-a), (6-a).or (3-b), (6-b) are solved for the steady or unsteady case respectively to obtain strengths of singularity on CRPs. Then the induced velocity \vec{V}_{FA} and \vec{V}_{AF} are calculated to renew the right-hand sides of (3-a), (6-a) or (3-b), (6-b) respectively. As soon as converged solutions of singularity strengths on two blade rows are obtained, hydrodynamic forces acting on them are computed. The thrust and torque coefficients of the fore propeller and the aft one are normalized by the fore propeller diameter and expressed as follows:

$$K_T = \frac{T_F + T_A}{\rho n^2 D_F^4}, K_Q = \frac{Q_F + Q_A}{\rho n^2 D_F^5}, K_{TF} = \frac{T_F}{\rho n^2 D_F^4},$$

$$K_{QF} = \frac{Q_F}{\rho n^2 D_F^5}, K_{TA} = \frac{T_A}{\rho n^2 D_F^4}, K_{QA} = \frac{Q_A}{\rho n^2 D_F^5} \quad (8)$$

Where T_F and T_A denote the thrust of the fore propeller and the aft one respectively, Q_F and Q_A are corresponding torque of two blade rows. n and D are the rotating velocity and diameter of the fore propeller, ρ is the density of water.

3 VALIDATIONS

3.1 Steady Cases

Experimental data related to the performance of CRPs operating in uniform flow are provided by Miller to validate the present method. The CRPs(CRP-4-0-4) are composed of a fore propeller DTMB3686, which is 4-bladed and left handed, and a aft propeller DTMB3687A, which is 4-bladed and right handed. The section of the propeller has NACA a=0.8 camber line and the modified NACA 66 thickness distribution. The main geometrical particulars of two blade rows can be seen in the reference [5](Miller 1976). The clearance between two stages is 0.1415 of the fore propeller diameter. The discretization of the blades is shown in Figure.2. The calculation results by present method are compared to the measured for a large range of advance ratios in Figure.3 to Figure.5.

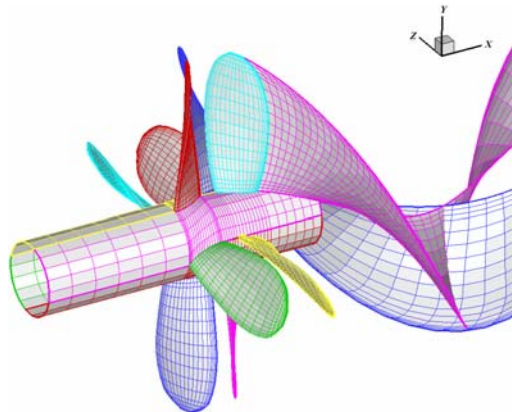


Figure.2 Coordinate system and discretization of CRP4-0-4

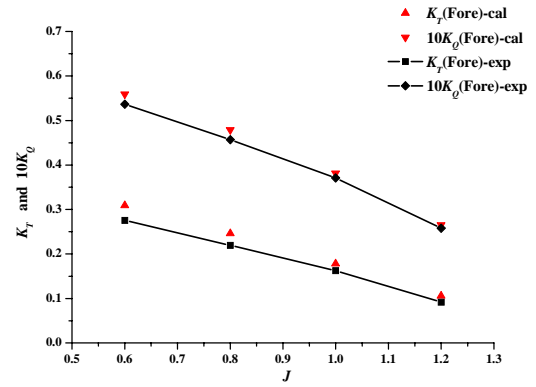


Figure.3 Thrust and torque of fore propeller of CRP-4-0-4 compared to experiment

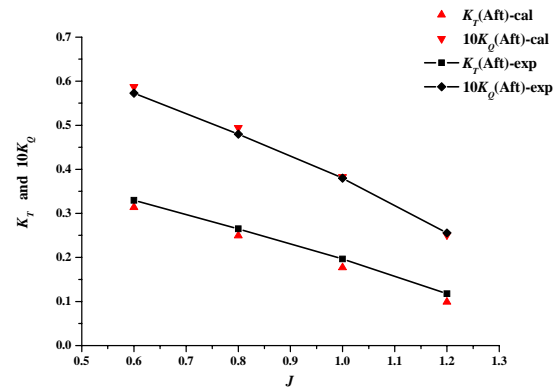


Figure.4 Thrust and torque of aft propeller of CRP-4-0-4 compared to experiment

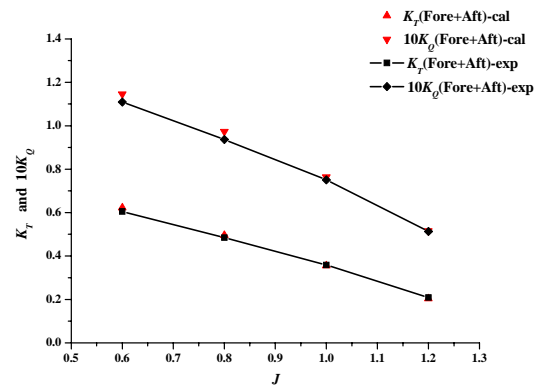


Figure.5 Total thrust and torque of CRP-4-0-4 compared to experiment

The CRPs(CRP-4-0-5) are composed of a fore propeller DTMB3686, which is 4-bladed and left handed, and a aft propeller DTMB3849, which is 5-bladed and right handed. The section of the propeller has NACA a=0.8 camber line and the modified NACA 66 thickness distribution. The main geometrical particulars of two blade rows can be also seen in the reference [5](Miller 1976). The clearance between two stages is 0.1415 of the fore propeller diameter. The discretization of the blades is shown in Figure.6. The calculation results by present

method are compared to the measured for a large range of advance ratios in Figure.7 to Figure.9.

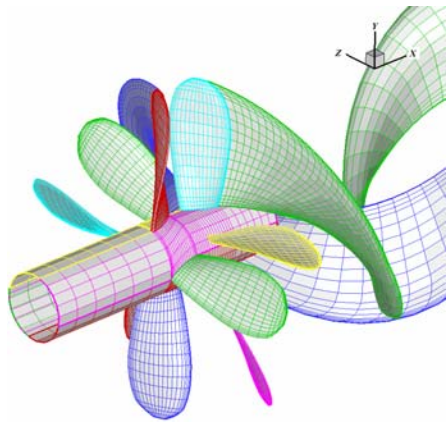


Figure.6 Coordinate system and discretization of CRP4-0-5

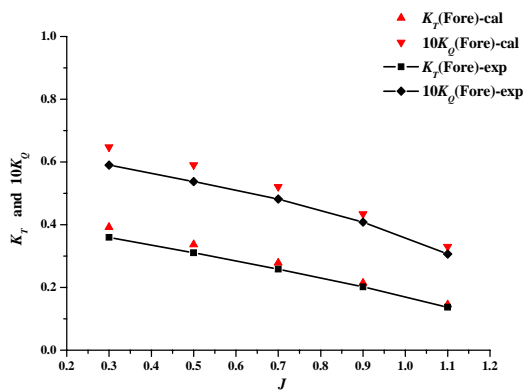


Figure.7 Thrust and torque of fore propeller of CRP-4-0-5 compared to experiment

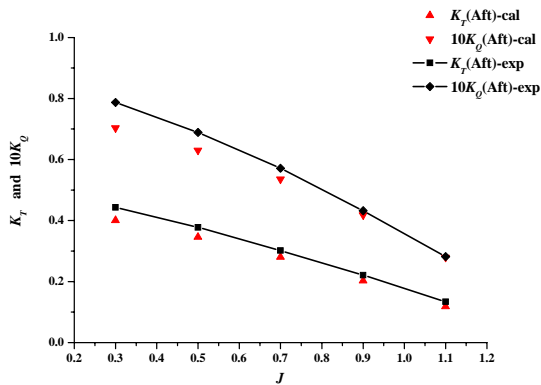


Figure.8 Thrust and torque of aft propeller of CRP-4-0-5 compared to experiment

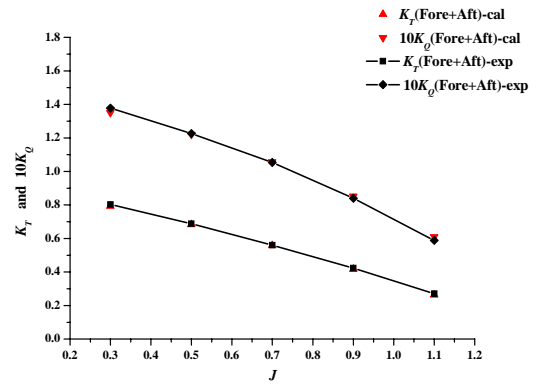


Figure.9 Total thrust and torque of CRP-4-0-5 compared to experiment

From the above two steady cases, the total thrust and torque predictions match well the measurements for a large range of advance ratios. However, there is a bigger discrepancy between the predicted and the measured for each body thrust and torque. It is no matching of the total load distribution in the calculation that leads to the fore calculated overpredicting the measurement and the aft calculated underpredicting the measurement. The adjustment of the hydrodynamic pitch angle can improve the prediction precision, however that should be based on a lot of numerical experiments.

3.2 Unsteady Cases

The hydrodynamic prediction is an unsteady problem in strict even in uniform flow. The inflow condition for the fore propeller or the aft one varies at each time step in time domain because of the interaction of the two propellers. The unsteady calculation for CRP4-0-4 and CRP4-0-5 are carried out for the design advance ratio in uniform flow.

The comparison of the numerical results of steady method and unsteady method with the experiment results are depicted in Figure.10. “stcal” denotes steady calculation and “uncal” denotes unsteady calculation. It is reasonable that steady calculation results are close to unsteady calculation results. In addition, CRPs have specific shaft frequency characteristic even in uniform flow. The unsteady prediction can capture the CRPs shaft frequency. For CRP-4-0-4, it has the unsteady thrust and torque at 8, 16, 24,... times the shaft frequency and no side forces and moments according to the reference[7] (M.Strasberg & Breslin 1976). Figure.11 and Figure.12 show the convergent results of thrust and torque of fore propeller and aft propeller respectively. Figure.13 to 15 give the harmonic amplitudes of the thrust and torque corresponding to 0, 8 and 16 times the shaft frequency, which has a big discrepancy comparing to the experiment especially for the aft propeller. It can be seen that the calculated harmonic amplitudes of thrust and torque are lower than the experiment results for the fore propeller and higher than the experiment results for the aft one at 8 times the shaft frequency. Comparing to the calculation results by the lifting surface method(LSD) according to

the reference [1](Tsakonas et al 1983), panel method has no advantage over it at high times the shaft frequency. Maybe that is caused by different wake models which are applied by panel method and lifting surface method respectively.

The comparison of the numerical results of steady method and unsteady method with the experiment results are depicted in Figure.16 for CRP-4-0-5. It can be seen that steady calculation results are close to unsteady calculation results and the unsteady calculation has a higher precision than the steady calculation. For CRP-4-0-5, the lowest frequency of thrust and torque appears at 40 times the shaft frequency and that of side forces and moments appears at 9 times the shaft frequency according to the reference [7](M.Strasberg & Breslin 1976). For the thrust and torque, the calculated amplitudes at the lowest frequency are very small and no experimental data are available for comparison. Figure.17 gives the average amplitudes of the total thrust and torque for CRP-4-0-5. Figure.18 gives the calculated harmonic amplitudes of the side forces and moments corresponding to 9 times the shaft frequency for CRP-4-0-5. Figure.17 shows that the calculation results by panel method agree with the experimental data and the calculation results by LSD. Figure.18 shows the same characteristic with CRP4-0-4 that the calculated amplitudes are lower than the experiment results for the fore propeller and higher than the experiment results for the aft one at 9 times the shaft frequency.

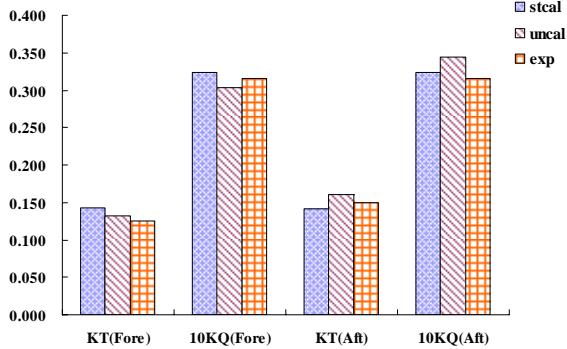


Figure.10 The comparison of the steady and unsteady prediction with experiment results for CRP4-0-4

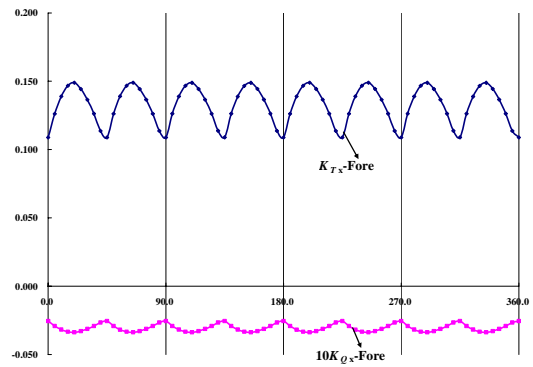


Figure.11 Total thrust and torque variation of fore propeller for CRP4-0-4

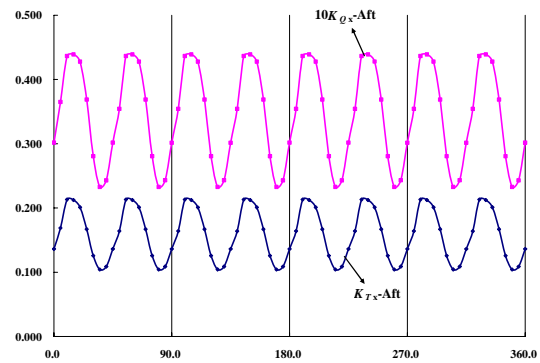


Figure.12 Total thrust and torque variation of aft propeller for CRP4-0-4

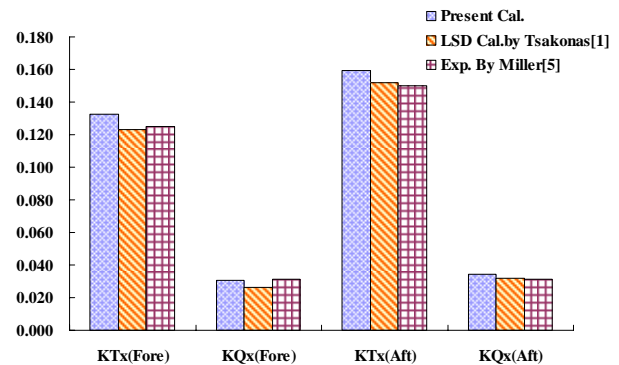


Figure.13 Average amplitude of total thrust and torque for CRP4-0-4

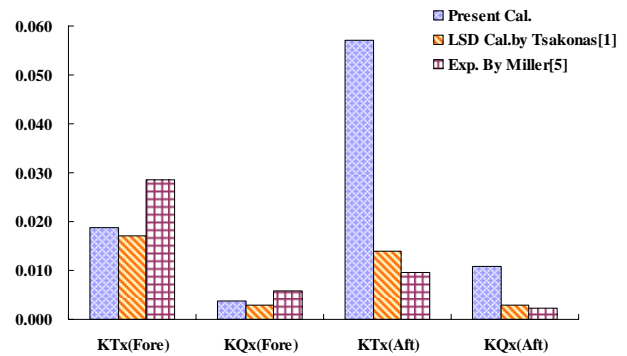


Figure.14 Harmonic amplitude of total thrust and torque of 8 times the shaft frequency for CRP4-0-4

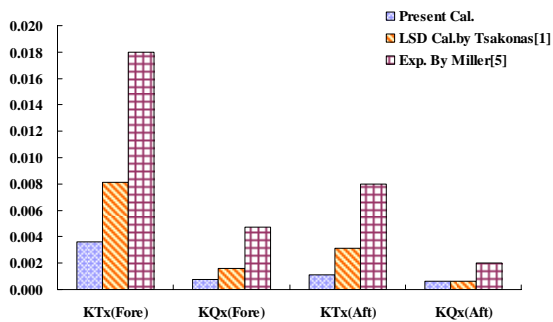


Figure.15 Harmonic amplitude of total thrust and torque of 16 times the shaft frequency for CRP4-0-4

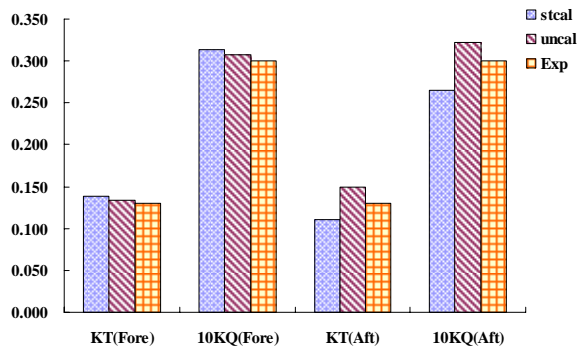


Figure.16 The comparison of the steady and unsteady prediction with experiment results for CRP4-0-5

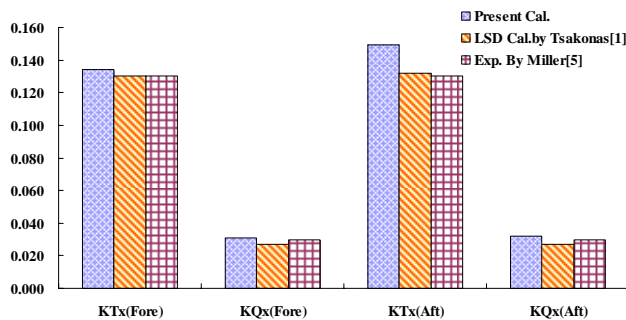


Figure.17 Average amplitude of total thrust and torque for CRP4-0-5

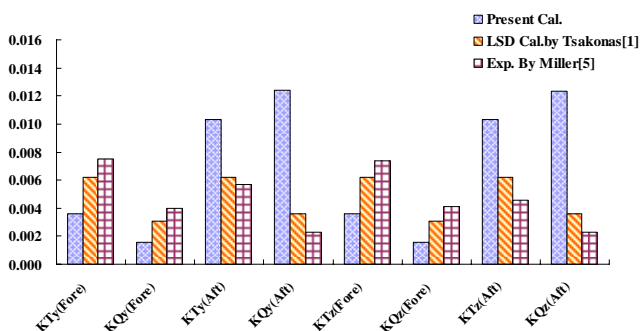


Figure.18 Harmonic amplitude of side forces and moments of 9 times the shaft frequency for CRP4-0-5

4 CONCLUSIONS

A general computational procedure established by using the potential based panel method has been developed to

predict the steady and unsteady performances of CRPs. The steady calculation results are encouraged and can be further improved by adjustment of wake model. The unsteady calculation results agree well with the steady calculation results for average amplitudes of thrust and torque. However, it has a big discrepancy comparing to the experimental data and the calculated results by LSD. The complicated wake model should be developed to improve the calculation precision. More validations with experiments, especially for the case in non-uniform flow, are required to assess the present method more thoroughly.

REFERENCES

- Tsakonas, W.R. Jacobs. (1983). 'Prediction of Steady and Unsteady Loads and Hydrodynamics Forces on Counterrotating Propellers'. *Journal of Ship Research* 27(3), pp.179-214.
- Yang C. J., Tamashima M., Wang G. Q., Yamazaki R. (1991). 'Prediction of the Steady Performance of Contra-Rotating Propellers by Lifting Surface Theory'. *Transactions of the West-Japan Society of Naval Architects* 82.
- Yang C. J., Tamashima M., Wang G. Q., Yamazaki R., Koizuka H. (1992). 'Prediction of the Unsteady Performance of Contra-Rotating Propellers by Lifting Surface Theory'. *Transactions of the West-Japan Society of Naval Architects* 83.
- Gu, H. & Kinnas, S.A. (2003). 'Modeling of Contra-Rotating and Ducted Propellers via Coupling of a Vortex-Lattice with a Finite Volume Method'. *Propellers/Shafting 2003 Symposium, Society of Naval Architects and Marine Engineers, Virginia Beach, U.S.A.*
- Miller, M.L. (1976). 'Experimental Determination of Unsteady Forces on Counterrotating Propellers in Uniform Flow', *David Naval Ship Research and Development Center Report SPD-659-01*.
- Miller, M.L. (1981). 'Experimental Determination of Unsteady Forces on Contrarotating Propellers for Application to Torpedoes'. *David Naval Ship Research and Development Center Report SPD-659-02*.
- M. Strasberg, & J.P. Breslin. (1976). 'Frequencies of the Alternating Forces due to Interactions of Contrarotating Propellers', *J. HYDRONAUTICS*, (10), pp.62-64.
- Hoshino. (1994). 'Experimental and Theoretical Analysis of Propeller Shaft Forces of Contra-Rotating Propellers and Correction with Full Scale Data'. *Propeller/Shafting'94 Symposium, Society of Naval Architects and Marine Engineers Virginia Beach, U.S.A.*
- Wang, G.-Q. & Hu, S.-G. (1988). 'Improvement of Prediction Method for Propeller Characteristics and Blade Pressure Distribution', *Selected Papers of*

Chinese Society of Naval Architects and Marine
Engineers (CSNAME) 3.